In situ fabrication and blueshifted red emission of GaN:Eu nanoneedles

Congkang Xu[1], Junghwan Chun[1], Bonghwan Chon[2], Taiha Joo[2] and Dong Eon Kim[1]

[1] Department of Physics and Electron Spin Science Center, Pohang University of Science and Technology, 790-784, Korea
[2] Department of Chemistry, Pohang University of Science and Technology, Pohang, 790-784, Korea

E-mail: kimd@postech.ac.kr

Abstract

A vapour transport route for the *in situ* fabrication of Eu-doped GaN nanoneedles is reported. The nanoneedles are single crystals of hexagonal structure and they grow in the [100] direction. The typical taper of a nanoneedle (in diameter) varies from 5 nm to 1 μm with a length of up to a few microns. Energy-dispersive x-ray studies indicate that the Eu concentration doped into the GaN nanoneedles is $\sim$0.2 at.%. Photoluminescence spectra show that the nanoneedles have very strong red emission around 611 nm with a significant blueshift by 11 nm probably due to the nanostructures' small size and the surface states of the nanoneedles. The flow rate of ammonia is shown to have a large effect on the doping rate and photoluminescence of GaN:Eu nanoneedles.

1. Introduction

The doping of one-dimensional (1D) GaN nanostructures has spurred ever-increasing interest because it enables one to realize various kinds of practical applications by tailoring the physical properties. Some works have already been reported, such as Mn- or Mn/Al-doped GaN nanowires, enabling one to achieve diluted magnetic semiconductor nanostructures for nanodevices in spintronics [1–3], Si-doped GaN nanowires resulting in the blue shift of ultraviolet (UV) emission [4, 5], P-doped GaN nanowires [6] and In-doped GaN nanowires [7]. However, most of the works have focused on 1D GaN nanostructures doped with transition elements and other elements, and the rare-earth (RE) elements have received little attention. Several studies on RE-doped GaN that have recently appeared were limited to films and powders [8–12], in which the visible and infrared light emission has been shown to be of importance for applications in electroluminescence devices [13, 14]. In particular, the $^5D_0$–$^7F_2$ intra-4f transition of trivalent Eu^{3+} ions seems most promising for attaining red light emission. True colour flat displays based on GaN:Eu films, which can be operated even under extreme conditions of temperature, humidity and radiation, have been demonstrated [11, 13–18] via robust visible red emission around 622 nm. 1D GaN nanostructures doped with RE elements are therefore expected to have more efficient luminescence at room temperature than their bare semiconductor hosts. They may offer a potential alternative for red light emission from a III-nitride nanodevice. No reports as yet are available for Eu-doped GaN nanoneedles. In this paper, we aim at the *in situ* growth of GaN:Eu single-crystalline nanoneedles via a simple and catalyst-free vapour transport route as well as at intense Eu red emission at room temperature.

2. Experiments

In situ Eu-doped GaN nanoneedle fabrication was carried out by placing an alumina boat loaded with a mixture of GaN powder (Aldrich, 99.99+%) and Eu_2O_3 power (Shanghai Chemicals Co. Ltd, 99.99%) with weight ratio of 4:1 and an α-Al_2O_3 substrate in a quartz tube furnace, as shown in figure 1(a). The boat was kept in the centre of a quartz tube with 25 mm diameter and 600 mm length heated zone in the furnace and then the sapphire substrate was placed 280 mm downstream from the boat. The base vacuum was kept at 95 mTorr. The furnace was heated to 1050 °C at a rate of 20 °C min^{-1} with a flow of high-purity ammonia gas (99.999%) at 80 or 150 sccm and then maintained at this
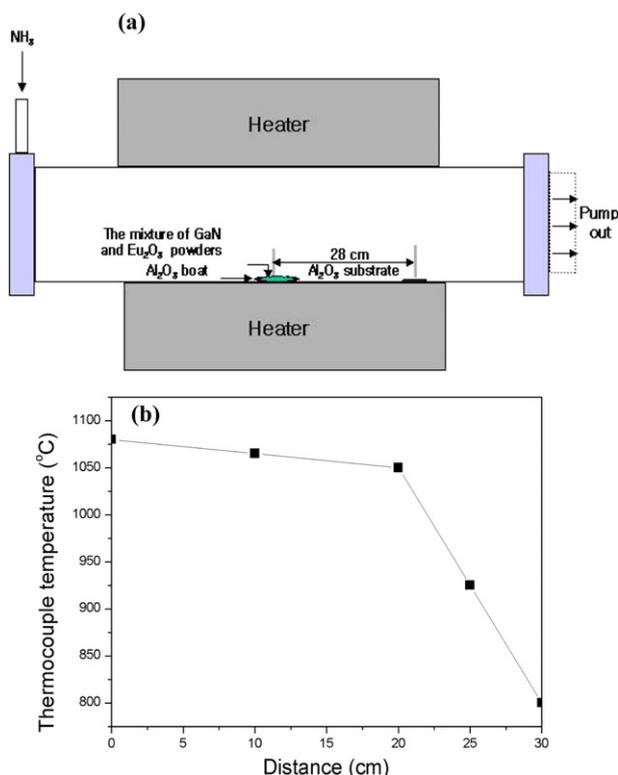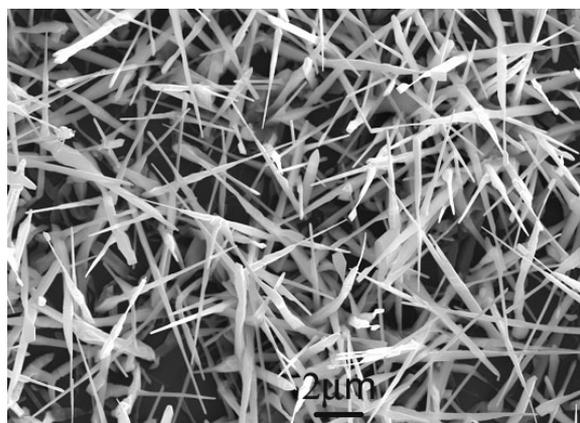
Figure 1. (a) Schematic diagram of the horizontal furnace used in the synthesis. (b) The temperature distribution curve in the furnace. (This figure is in colour only in the electronic version)

Figure 2. SEM images of the as-obtained GaN:Eu nanoneedles.

Figure 3. XRD pattern of GaN:Eu nanoneedles.

temperature for 60 min, and the quartz tube pressure was kept at 500 Torr. The temperature distribution is shown in figure 1(b). After the system was cooled with NH_3, wool-like light-yellow coloured products were obtained from the sapphire substrate. In order to gain further insights into the optical properties of the GaN:Eu nanoneedles, undoped GaN nanowires had been prepared under identical conditions, but without Eu_2O_3. The high purity of the samples is ensured since they were produced in a bulk quantity by a simple, one-step and catalyst-free process.
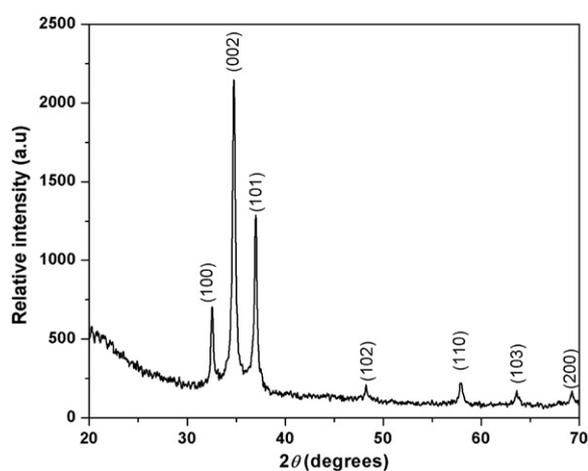
The as-obtained samples were investigated by x-ray diffraction (XRD, Japanese Rigaku). The morphology and size distribution of the nanoneedles were characterized using a scanning electron microscope (SEM, Hitachi H-8010), and a transmission electron microscope (TEM, JEOL-2010) equipped with energy-dispersive x-ray (EDX) spectroscopy. Photoluminescence (PL) measurement was performed using the third harmonic of a cavity-dumped femtosecond Ti:sapphire laser at 266 nm with an output power of 10 mW and a repetition rate of 13 kHz. As a comparison, the PL spectra of undoped GaN nanowires were also recorded under identical experimental conditions.

3. Results and discussion

Figure 2 shows the SEM image of the as-obtained samples having a needle-like nanostructure grown on the sapphire substrate. The nanoneedles are densely distributed over the whole substrate. Typically the taper of a nanoneedle (in diameter) varies from 5 nm to 1 μm, with a length of up to a few microns.

Figure 3 shows an XRD pattern of the as-obtained samples with a flow rate of ammonia at 80 sccm. The diffraction peaks are quite similar to those of bulk GaN with the hexagonal wurtzite structure ($a = 3.18$ Å, $c = 5.18$ Å). The diffraction data are in good agreement with published values [5] for GaN nanowires. No typical diffraction peaks corresponding to Eu or Eu compound impurity phases such as GaEu and EuN are observed. The strong intensities of the peaks relative to the background show that the nanoneedles are well crystallized.
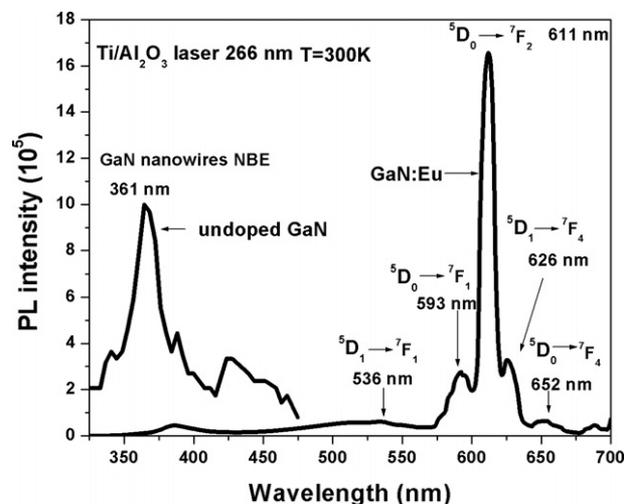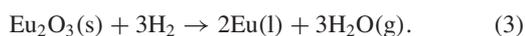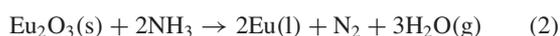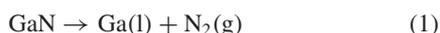
Figure 4(a) shows a TEM image of a nanoneedle of $\sim$85 nm diameter and $\sim$4 μm length. The EDX analysis (lower inset) indicates that the nanoneedle is mainly composed of Ga and N with an atomic ratio of 54:46 and a small trace of Eu. The atomic ratio of Ga to Eu is about 99.8:0.2. The selected area electron diffraction (SAED) pattern (upper inset) does not show any four-fold symmetry pattern which would be present if either tetragonal or cubic phases such as $EuGa_4$ and EuN were formed in the nanoneedles. Instead, the diffraction spots show only the six-fold symmetry with a [001] zone axis, indicating that GaN:Eu nanoneedle is a single crystal of hexagonal structure GaN and grows in the [100] direction. Figure 4(b) exhibits a typical high-resolution TEM (HRTEM)
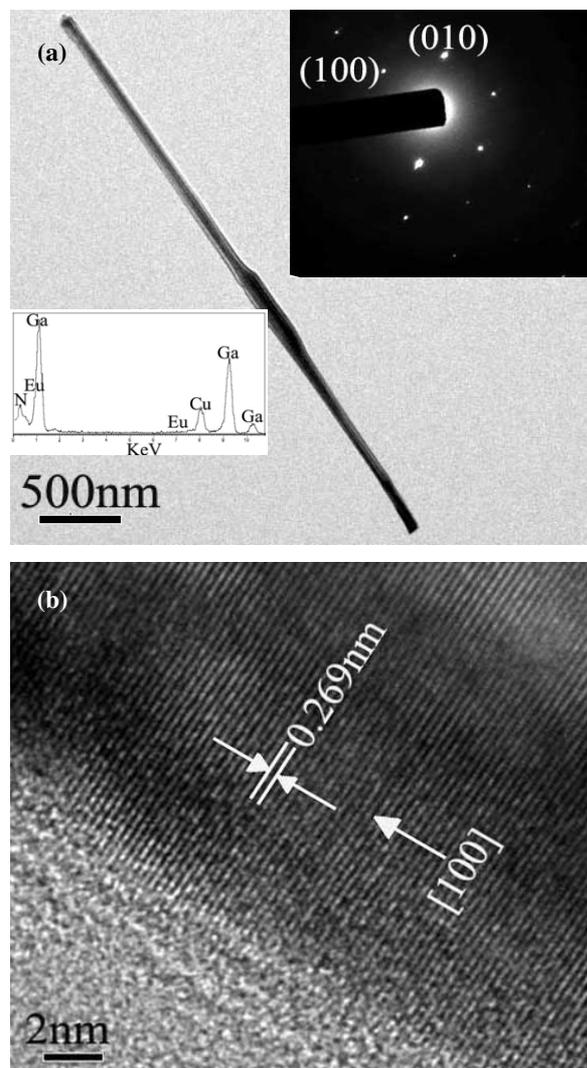
Figure 4. (a) A TEM image of an individual nanoneedle; the insets are the SAED pattern and EDX spectrum; (b) an HRTEM image of the corresponding nanoneedle.

image of the corresponding nanoneedle. The spacing between the lattice planes perpendicular to the nanoneedle axis is about 0.269 nm, which agrees with the (100) spacing of wurtzite GaN, further confirming the growth direction of the nanoneedle to be [100]. The clear fringes indicate no secondary phase within GaN:Eu nanoneedles. However, it is difficult to exclude the presence of Eu on the surface and/or near-surface region because of the indistinct surface.

There are probably several chemical reactions involved in our method to fabricate GaN:Eu nanoneedles in the temperature range from 800 to 1050 °C. GaN can be decomposed into Ga and N_2, and Eu_2O_3 will be reduced to Eu since NH_3, besides acting as a nitrogen source, can decompose stepwise to NH_2, NH, H_2 and N_2 at temperatures above 800 °C.

$$GaN \rightarrow Ga(l) + N_2(g) \qquad (1)$$

$$Eu_2O_3(s) + 2NH_3 \rightarrow 2Eu(l) + N_2 + 3H_2O(g) \qquad (2)$$

$$Eu_2O_3(s) + 3H_2 \rightarrow 2Eu(l) + 3H_2O(g). \qquad (3)$$

Figure 5. Room-temperature PL spectra of undoped GaN nanowires and Eu-doped GaN nanoneedles excited by the third harmonic at the 266 nm line of a Ti/Al_2O_3 laser.

Eu can be incorporated into Ga to form Ga/Eu, which is carried away from the hot zone by the carrier gas and then deposits onto the Al_2O_3 substrate ($\sim$780 °C, growth area). So the following reaction occurs:

$$2Ga/Eu + 2NH_3 \rightarrow 2GaN/Eu + 3H_2. \qquad (4)$$

When the GaN concentration reaches saturation in the Ga–Eu droplet, solid GaN will segregate at the droplet–substrate interface. Thus, the Ga–Eu droplet acts both as a nucleation site for GaN segregation and as a medium to incorporate Eu into GaN. Finally, GaN:Eu nanoneedles are formed. This process is similar to that in Si-doped GaN nanowires [5]. It is noteworthy that in the present study we obtained nanoneedles instead of nanowires. It is believed that the formation of nanoneedles is in association with surface energy and growth conditions as reported previously [19]. NH_2, NH and H_2 stemming from the decomposition of NH_3 may exist as intermediates at the surface of GaN:Eu. The absorption of H or NH_2/NH on the surface of GaN:Eu possibly saturates Ga and N dangling bonds and reduces the surface energy [20], leading to the growth of GaN:Eu nanoneedles. Further investigation is required.

Figure 5 shows room-temperature PL spectra of undoped GaN nanowires and Eu-doped GaN nanoneedles grown on Al_2O_3 substrate by the vapour transport route using the third harmonic at 266 nm of a cavity-dumped femtosecond Ti:sapphire laser with an output of 0.3 mW and a repetition rate 13 kHz. The undoped GaN nanowires exhibit intrinsic luminescence at 361 nm. The Eu-doped GaN nanoneedles show an extremely strong red emission at 611 nm, which can be assigned to the energy transition from $^5D_0$ to $^7F_2$ of the E^{3+} inner 4f shell. The weak PL peaks at 536, 593 and 652 nm are in association with the transitions from $^5D_1$ to $^7F_1$, $^5D_0$ to $^7F_1$ and $^5D_0$ to $^7F_3$, respectively. These peaks are similar to those observed in GaN:Eu film [11] and powder [12] except for the blue shift of the peak positions. The peak at 626 nm is probably due to the energy level transition from $^5D_1$ to $^7F_4$, which is consistent with the

results reported [11, 16]. Interestingly, the PL intensity of Eu emission from GaN:Eu nanoneedles in which only weaker near band edge emission and yellow band emission occur is very strong and comparable to the intrinsic emission of undoped GaN nanowires. The main emission of Eu^{3+} at 611 nm is significantly blueshifted by ∼11 nm as compared with the GaN:Eu films [11] and powders [12]. The excitation source for PL should be taken into account to make sure that this blueshift is due to the nanostructures. Although we used an above-bandgap excitation source (266 nm) unlike [11] and [12], where the excitation is at 325 nm, experimental investigations with different excitation sources such as above-bandgap (He–Cd laser 325 nm, Ar^+ laser 336, 355, and 363.8 nm; Xe lamp 356 nm) and below-bandgap (Ar^+ laser 457.9 and 460 nm, Xe lamp 385 nm) ones for the PL of GaN:Eu films [11, 21] and powders [12] showed that the main emission position of Eu^{3+} is nearly independent of the excitation source. Importantly, the energy splitting and transition of 4f levels of RE ions depend on the crystal field of the host matrix [22]. It has been shown that the crystallinity and size of the host matrix affect the main emission line of Eu^{3+} causing a significant blueshift. In the case of Eu-doped ZrO_2 nanoparticles, the blueshifts were 10 nm and 17 nm for diameters of 30 nm and 14 nm, respectively [23]. In the present work, the near band edge emission (361 nm) of the undoped GaN nanowires has a blueshift of ∼2 nm as compared with that of undoped GaN film (363 nm), indicating that the undoped GaN nanowires are of high quality. Moreover, as determined from the TEM study, the GaN:Eu nanoneedles are almost defect-free single crystals. The average diameter of the nanoneedles is comparable to that of Eu-doped ZrO_2 nanoparticles [23]. This one-step, simple and catalyst-free synthesis process for making GaN:Eu nanoneedles also ensures the high purity of as-obtained samples. Hence we believe that the blueshift in this work is not the result of the excitation source at 266 nm, but, rather, is intrinsic because of the nanostructures (high purity, crystallinity, size, etc) of the GaN:Eu nanoneedles. Kudrawiec *et al* [24] also found that emission (at 616 nm) of GaN:Eu nanoparticles (∼7 nm) is blueshifted by 6 nm as compared with bulk GaN:Eu (at 622 nm). Furthermore, by investigating the aggregation of nanometre grains into micrometre-sized conglomerates, they concluded that surface states play a significant role in the photoluminescence. In this work, the diameter of the nanoneedle varies from 5 nm to 1 μm along the growth direction, which may be viewed as the combination of nanoparticles and micrometre-sized conglomerates. Hence, besides small-size nanostructures causing a confinement effect, the surface states are likely responsible for the change in GaN:Eu nanoneedles. On the other hand, other factors such as strain and thermal heating effects may have an effect on the variation in PL.

The flow rate of ammonia also has a significant effect on the photoluminescence of the GaN:Eu nanoneedles. It is well accepted that the V/III ratio has an effect on the GaN crystalline quality and RE-related emission in GaN [11, 25]. In the present work, it is reasonably believed that the variation in NH_3 flow rate is similar to the change in V(N)/III(Ga). Figure 6 shows two room-temperature PL spectra of GaN:Eu nanoneedles grown at 80 and 150 sccm of NH_3. The intensities of the Eu main emission peaks at 611 and 626 nm decrease
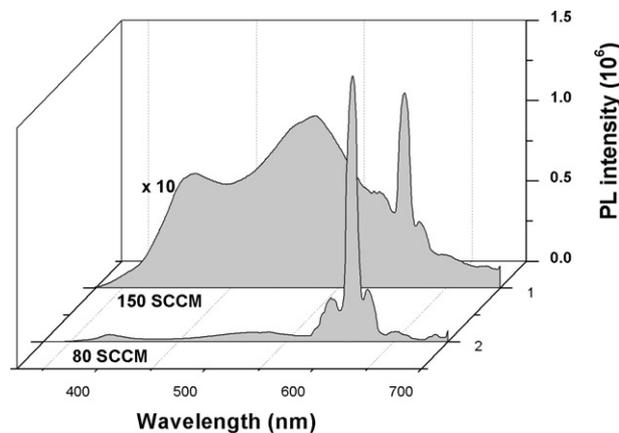
Figure 6. PL spectra of GaN:Eu nanoneedles showing the dependence on the flow rates of ammonia.

significantly with increasing NH_3 flow rate. Unexpectedly, the value of Eu in the sample fabricated at a 150 sccm of NH_3 was unavailable by EDX because of the detection limit, indicating that the Eu concentration at 150 sccm is much lower (or at least less than the detection limit) than that at 80 sccm. In a sense, the Eu concentration decreases while increasing the NH_3 flow rate (N/Ga). This trend in Eu content in part expounds the similar trend in Eu PL intensity versus N/Ga ratio, consistent with the previous report [26], where the enhanced PL intensity in low NH_3 flow rate could be due to the increase of Eu concentration and of the nitrogen vacancy complex which plays an important role in energy transfer from GaN to Eu. The intensity of red emission at 622 nm is mainly dependent on the number of Eu occupying Ga sites [11, 25]. As to why the amount of Eu in the nanoneedles depends on NH_3, there are two possible explanations for the variation in Eu concentration with NH_3 flow rate: (i) low NH_3 flow rate or relatively Ga-rich growth conditions at which good crystalline GaN is usually grown [27] enables the incorporation of a large amount of Eu; (ii) site competition between Eu and Ga atoms gives rise to a decreased incorporation of Eu atoms while the NH_3 flow rate is increased. In addition, a low NH_3 flow rate facilitates nitrogen vacancies in the GaN crystal and enhances the PL intensity [26].

4. Conclusions

Taken together, a vapour transport route for the *in situ* fabrication of Eu-doped GaN nanoneedles is presented. The nanoneedles are single crystalline with hexagonal structure and grow in the [100] direction. EDX analyses show that the Eu concentration doped into the GaN nanoneedles is ∼0.2 at.%. PL spectra show that the nanoneedles have very strong red emission around 611 nm with a significant blueshift by 11 nm probably due to the nanostructures' small size and the surface states of the nanoneedles. The flow rate of ammonia is shown to have a large effect on the doping rate and photoluminescence of GaN:Eu nanoneedles. This nanostructure may offer a potential alternative for red light emission from a III-nitride nanodevice.

Acknowledgments

References

[1] Han D, Park J, Rhie K, Kim S and Chang J 2005 *Appl. Phys. Lett.* **86** 032506

[2] Choi H, Seong H, Chang J, Lee K, Park Y, Kim J, Lee S, He R, Kuykendall T and Yang P 2005 *Adv. Mater.* **17** 1351

[3] Xu C K, Chun J, Rho K, Kim D E, Kim B J, Yoon S, Han S E and Kim J J 2006 *J. Appl. Phys.* **99** 064312

[4] Liu J, Meng X M, Jiang Y, Lee C S, Bello I and Lee S T 2003 *Appl. Phys. Lett.* **83** 4241

[5] Xu C K, Chung S, Kim M, Kim D E, Chon B, Hong S and Joo T 2005 *J. Nanosci. Nanotechnol.* **5** 530

[6] Liu B D, Bando Y, Tang C C, Xu F F and Golberg D 2005 *J. Phys. Chem.* B **109** 21521

[7] Dai L, Liu S F, You L P, Zhang J C and Qin C G 2005 *Nanotechnology* **17** L445

[8] Heikenfeld J, Garter M, Lee D S, Birkhahn R and Steckl A J 1999 *Appl. Phys. Lett.* **75** 1189

[9] Lozykowski H J, Jadwisienczak W M, Han J and Brown I G 2000 *Appl. Phys. Lett.* **77** 767

[10] Li Z, Bang H, Piao G, Sawahata J and Akimoto K 2002 *J. Cryst. Growth* **240** 382

[11] Pan M and Steckl A J 2003 *Appl. Phys. Lett.* **83** 9

[12] Wu H, Poitras C B, Lipson M, Spencer M G, Hunting J and Disalvo F J 2006 *Appl. Phys. Lett.* **88** 011921

[13] Steckl A J and Zavada J M 1999 *MRS Bull.* **24** 33

[14] Steckl A J, Heikenfeld J C, Lee D S, Garter M J, Baker C C, Wang Y and Jones R 2002 *IEEE J. Sel. Top. Quantum Electron.* **8** 749

[15] Nyein E E, Hommerich U, Heikenfeld J, Lee D S, Steckl A J and Zavada J M 2003 *Appl. Phys. Lett.* **82** 1655

[16] Monteiro T, Boemare C, Soares M J, Sa Ferreira R A, Carlos L D, Lorenz K, Vianden R and Alves E 2001 *Physica* B **308–310** 22

[17] Bang H, Morishima S, Li Z, Akimoto K, Nomura M and Yagi E 2002 *J. Cryst. Growth* **237–239** 1027

[18] Morishima S, Maruyama T, Tanaka M, Masumoto Y and Akimoto K 1999 *Phys. Status Solidi* a **176** 113

[19] Hiruma K, Yazawa M, Haraguchi K, Ogawa K, Katsuyama T, Koguchi M and Kakibayashi H 1993 *J. Appl. Phys.* **74** 3162

[20] Northrup J E, Felice R D and Neugebauer J 1997 *Phys. Rev.* B **56** R4352

[21] Wang K, Martin R W, O'Donnell K P, Katchkanov V, Nogales E, Lorenz K, Alves E, Ruffenach S and Briot O 2005 *Appl. Phys. Lett.* **87** 112107

[22] Nakanishi Y, Wakahara A, Okada H, Yohida A, Ohshimara T, Itoh H, Nakao S, Saito K and Kim Y T 2003 *Nucl. Instrum. Methods Phys. Res.* B **206** 1033

[23] Gutzov S, Bredol M and Wasgestian F 1998 *J. Phys. Chem. Solids* **59** 69

[24] Kudrawiec R, Nyk M, Podhorodecki A, Misiewicz J, Strek W and Wolcyrz M 2006 *Appl. Phys. Lett.* **88** 061916

[25] Hite J, Thaler T, Khanna R, Abernathy C R, Pearton S J, Park J H, Steckl A J and Zavada J M 2006 *Appl. Phys. Lett.* **89** 132119

[26] Sawahata J, Seo J W, Takiguchi M, Saito D, Nemoto S and Akimoto K 2006 *Phys. Status Solidi* c **3** 1911

[27] Calleia E, Sanchez-Garcia M A, Sachez F J, Calle F, Naranjo F B, Munoz E, Jahn U and Ploog K 2000 *Phys. Rev.* B **62** 16826